



Global Advanced Research Journal of Agricultural Science (ISSN: 2315-5094) Vol. 7(6) pp. 176-182, June, 2018 Issue.
Available online <http://garj.org/garjas/home>
Copyright © 2018 Global Advanced Research Journals



Full Length Research Paper

Nanoparticles and antifungal activity of iron sulfide synthesized by green route using *Uncaria tomentosa* leaves extract

Nidá M. Salem¹, Fatin M. Abedalaziz² and Akl M. Awwad^{1,2*}

¹Department of Plant Protection, School of Agriculture, the University of Jordan, Amman, Jordan

²Department of Materials Science, Royal Scientific Society, Amman, Jordan

Accepted 18 January, 2018

This research paper described the synthesis of iron sulfide nanoparticles from iron nitrate and sodium sulfide in the presence of *Uncaria tomentosa* leaves aqueous extract at ambient temperature. The iron sulfide nanoparticles (FeSNPs) were characterized by X-ray diffraction (XRD), transmission electron microscopy (TEM), energy-dispersive X-ray spectroscopy (EDS), UV-visible spectroscopy (UV-vis) and Fourier transform infrared spectroscopy (FT-IR) techniques. The synthesized FeSNPs were found to be spherical in shape with average size diameter 40nm. Iron sulfide nanoparticles exhibited strong antifungal activity towards plant pathogenic fungus, *Fusarium oxysporum* f.sp. *lycopersici*. These results led us to extend our research to study the effect of FeSNPs on the control of *Fusarium* wilt in tomato crops as fungicide and plant growth.

Keywords: iron sulfide nanoparticles • *Uncaria tomentosa* leaves extract • Antifungal activity • *Fusarium oxysporum*

INTRODUCTION

The present study was designed to synthesize iron sulfide nanoparticles (FeSNPs) by facile green method from sodium sulfide nonahydrate ($\text{Na}_2\text{S}\cdot 9\text{H}_2\text{O}$) and iron nitrate nonahydrate [$\text{Fe}(\text{NO}_3)_3\cdot 9\text{H}_2\text{O}$] in the presence of *U. tomentosa* leaves aqueous extract at ambient temperature. Different routes and methods have been developed to synthesize iron sulfides nanoparticles, such as solvothermal process (Kar and Chaudhuri 2005; Zhao et al., 2009). polyol mediated process (Ivantsov et al., 2017), microbial synthesis (Kim et al., 2015; Zhou et al., 2017), hydrothermal synthesis (Pua et al., 2010; Akhoondi et al.,

2013), sulfurization of hematite nanowires (Cummins et al., 2013), chemical precipitation method (Kim et al., 2011; Liu et al., 2017), a single source precursor approach (Zhang et al., 2010), chemical bath deposition (Akhtar et al., 2015), high-energy mechanical milling and mechanochemical processing (Chin et al., 2005), microwave synthesis (Xiao et al., 2016), from dithiocarboxylate precursor complex decomposition (Maji et al., 2012), from natural pyrite (Ding et al., 2013).

In this study, we report for the first time a novel, rapid, cost-effective and environmentally biosynthesis of iron sulfide nanoparticles using *U. tomentosa* leaves extract at ambient temperature. This biosynthetic green route for iron sulfide nanoparticles was found to be extremely effective against

*Corresponding Author's Email: akl.awwad@yahoo.com

fungal plant pathogen, *Fusarium oxysporum* f.sp. *lycopersici*.

MATERIALS AND METHODS

MATERIALS

The precursors iron nitrate nanahydrate [$\text{Fe}(\text{NO}_3)_3 \cdot 9\text{H}_2\text{O}$, $\geq 99.95\%$] and sodium sulfide nanahydrate [$\text{Na}_2\text{S} \cdot 9\text{H}_2\text{O}$, $\geq 99.99\%$] were purchased from Sigma-Aldrich. *U. tomentosa* leaves were collected from the campus of Royal Scientific Society, Amman, Jordan. Distilled water was used in all experimental work.

Preparation of *U. tomentosa* leaves aqueous extract

U. tomentosa leaves were washed three times with distilled water to remove dust. Afterwards, leaves left to dry in shade for two weeks and crushed for small pieces. 20g of crushed leaves were placed in 400ml distilled water and boiled for 10min. Afterwards, the aqueous mixture filtered using Whitman filter paper No. 1 to obtain the yellow aqueous extract. The filtrate was kept in glass bottle with tight cover at room temperature for synthesis of FeS nanoparticles.

Iron sulfide nanoparticles synthesis

In a typical synthesis method, 2g of iron nitrate nonahydrate ($\text{Fe}(\text{NO}_3)_3 \cdot 9\text{H}_2\text{O}$) was dissolved in 100 ml *U. tomentosa* leaves aqueous extract under magnetic stirring at ambient temperature for 5min. when the color of the solution changed from pale yellow to deep brown color, sodium sulfide nonahydrate ($\text{Na}_2\text{S} \cdot 9\text{H}_2\text{O}$) solution was added to *U. tomentosa*/iron nitrate mixture drop wise, the color of reaction mixture started changing to homogenous grey-black suspended particles, indicating the formation of monodispersed iron sulfide nanoparticles. The suspended particles were separated by centrifugation at 1500 rpm/min for 5min and repeatedly washed with distilled water to remove any biological materials. Iron sulfide nanoparticles after purification were dried in a vacuum at 60°C for FT-IR, XRD, SEM-EDS and TEM analysis.

Characterization techniques

Synthesized FeSNPS were characterized by X-ray diffraction (Shimadzu, XRD-6000), Transmission electron microscopy spectroscopy (JEM-2100, JEOL Co.) coupled with selected area electron diffraction (SED). UV-vis spectroscopy (SPUV-26, Sco-tech) and Fourier transform infrared spectroscopy (Shimadzu, IR-Prestige-21).

Antifungal activity of FeSNPs

The antifungal activity of FeSNPs was performed by agar well diffusion method. The green synthesized FeSNPs were evaluated against plant pathogens such as *Fusarium oxysporum* f.sp. *lycopersici*. The molten Potato Dextrose Agar (PDA) consists of four discs. Amphotericin B was used as positive control. Each test was repeated three times to ensure reliability.

RESULTS AND DISCUSSION

X-ray diffraction (XRD) analysis

XRD profile of green synthesized iron sulfide nanoparticles, **Figure 1** indicated the coexistence of two different structures. The diffraction peaks at $2\theta = 12.21^\circ$, 15.96° , and 30.24° correspond to the (011), (111), and (102), respectively, which indicate the presence FeS nanocrystals (JCPDS File No. 76-0964). The average particle size calculated using the Debye-Scherrer equation (Ghidan et al., 2016).

$$D = 0.9\lambda/\beta \cos\theta$$

Where D is the crystalline size diameter; λ is the wave length of x-ray (1.4506Å), β is the value of full width at half maximum, and θ is the Bragg's angle. The value of D was obtained for biosynthesized FeSNPs is 20nm.

Fourier Transform infrared (FT-IR) analysis

FT-IR spectrum of *U. tomentosa*, **Figure 3** showed a number of peaks thus reflecting its complex nature. Strong broad absorption band at 3383 cm^{-1} is characteristic of the alcohol/phenol –OH stretching vibration, carboxylic acid –OH stretch and N-H stretching of amides. Absorption bands at 2924 cm^{-1} and 2850 cm^{-1} can be ascribed to the stretching mode of CH_3 and CH_2 . The peak located at 1739 cm^{-1} could be assigned to the C=O stretching in the carboxyl or C=N bending in the amide groups. Peak at 1612 cm^{-1} is characterized to –NH stretch of primary amines. Peaks at 1442 cm^{-1} and 1230 cm^{-1} are characterized –NH in secondary amines, aromatic –CH stretching vibrations, and C-C-N amines. Strong peak at 1064 cm^{-1} indicated the stretching vibration of (NH)–C–O group. Peaks at $\sim 621\text{ cm}^{-1}$ refers to O=C=O bending in carboxylic acids, N–C=O, and C–N–C bending mines. FT-IR spectrum of synthesized FeSNPs, FT-IR spectrum of the synthesized FeSNPs, **Figure 4** showed the strong bands at $671\text{--}428\text{ cm}^{-1}$ which is attributed to the vibrations of elongation and of deformation of vibratory FeS. The broad absorption peak at $3479\text{--}3321\text{ cm}^{-1}$ corresponds to O–H

Graphical Abstract

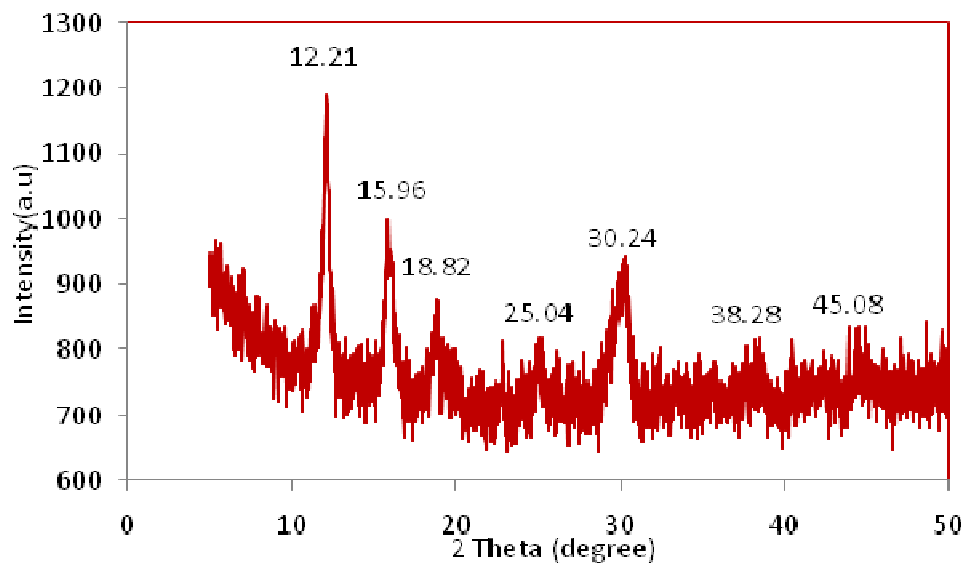
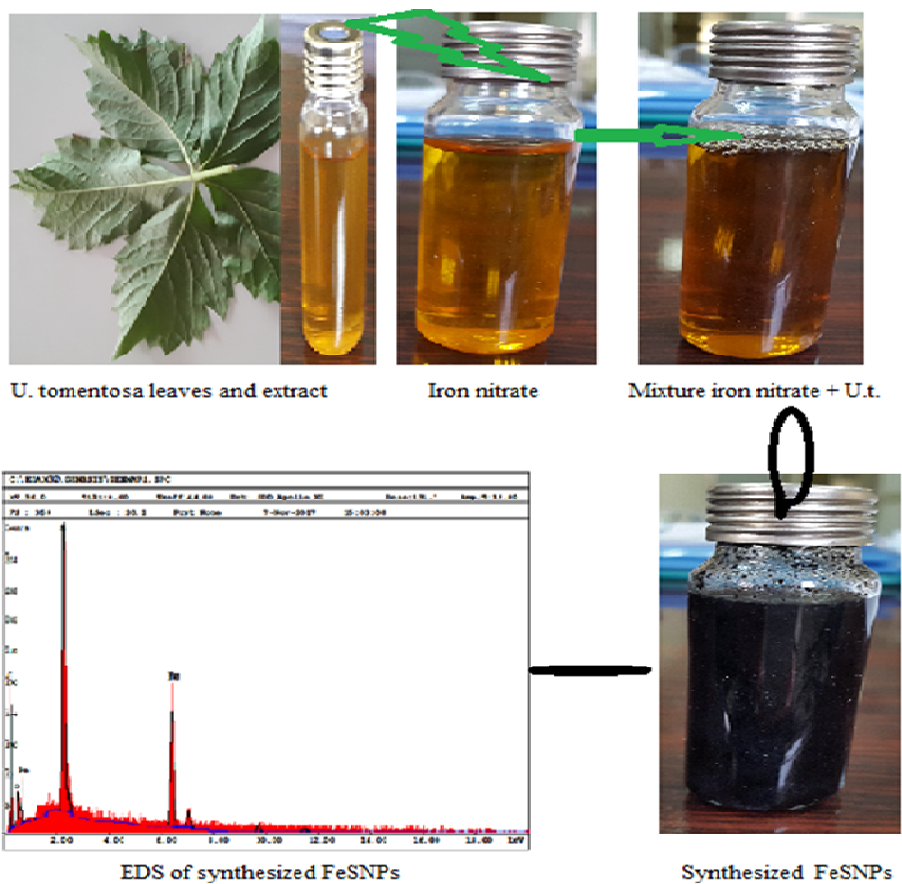


Figure 2 XRD pattern of synthesized FeS nanoparticles.

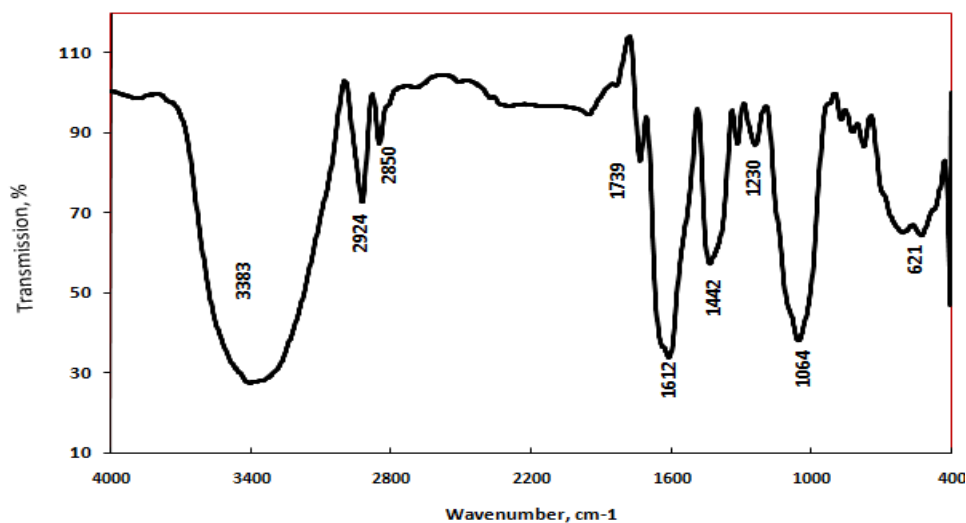


Figure 3 FT-IR of *U. tomesota* leaves extract

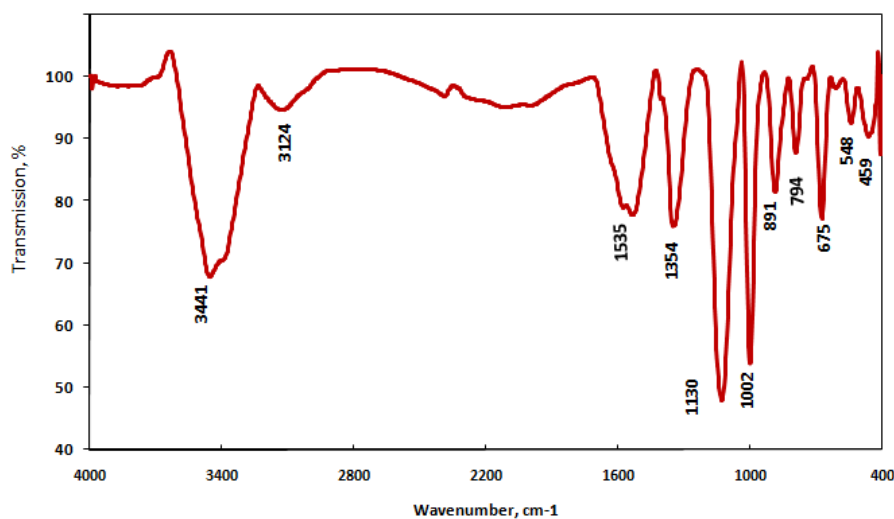


Figure 4 FT-IR of synthesized FeSNPs

stretching mode arising from the absorption of water on the surface of FeSNPs. The structural changes in FT-IR spectra indicated that the capping and stabilization of iron sulfide nanoparticles via the coordination with OH, -NH, C=O, C=N. The physicochemical properties of *U. tomesota* leaves extract act as capping agent and prevents the nanoparticles formed from aggregation.

UV-vis spectroscopy analysis

The surface plasmon vibrations (SPR) of iron sulfide nanoparticles produced a peak centered around 312nm,

Figure 5. No UV-Vis peaks appeared due to the aqueous extract of *U. tomentosa* leaves.

Transmission electron microscopy (TEM) analysis

Typical TEM micrograph for as prepared FeSNPs is shown in **Figure 6**. The TEM micrograph clearly showed nanostructure homogeneities with spherical morphologies of FeSNPs. The TEM observation showed the nanospheres with an average diameter of 40nm. This slight deviation of the particle size estimation compared to that calculated from XRD analysis can be attributed to the deviation of the spherical shape of the particles that is required for the

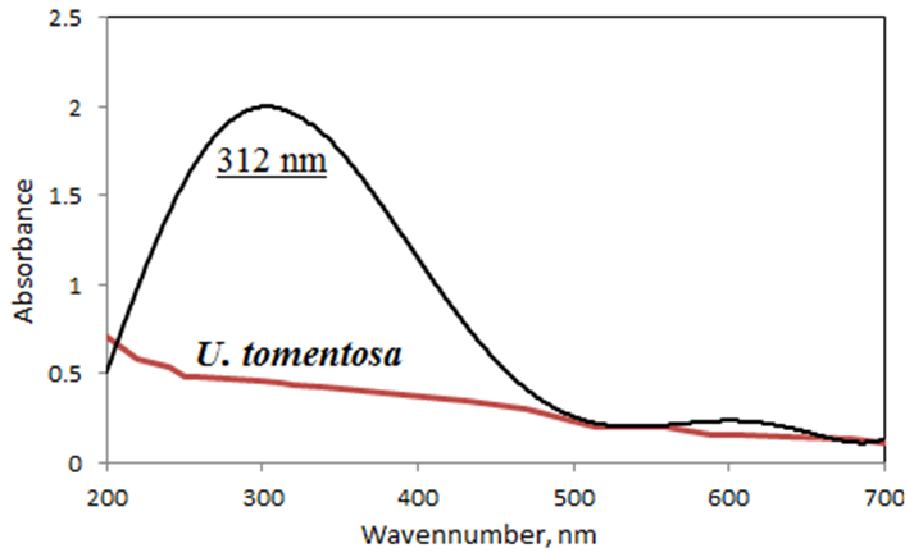


Figure 5 UV-vis. Spectrum of synthesized FeSNPs and plant extract

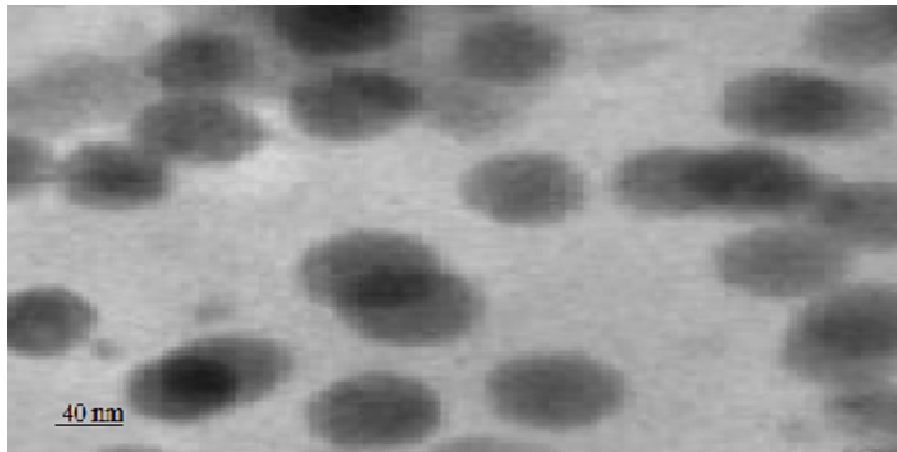


Figure 6. TEM images of synthesized FeSNPs using *U. tomentosa* leaves aqueous extract

Debye–Scherrer formula and the detection limit of the XRD diffractometer. Energy-dispersive X-ray spectroscopy (EDS) profile of the synthesized iron sulfide nanoparticles is illustrated in **Figure 7**.

Antifungal activity FeSNPs against *F. oxysporum*

The antifungal inhibitory effect on the growth was investigated under different concentrations of FeSNPs by a well diffusion assay on a Potato Dextrose Agar (PDA) plates. It was observed that iron sulfide nanoparticles have antifungal activities at different concentrations. The maximum inhibitory activity of $40\text{ppm} \pm 10\text{ppm}$ ZOI was obtained and increased slightly at 80 and 100ppm concentrations of FeSNPs. No inhibition zone were observed using the aqueous extract of *U. tomentosa* leaves. Present study observed results reveal that the green

synthesized FeSNPs showed a significant effect as antifungal towards plant pathogen *F. oxysporum* compared with positive drug control. It could be explained by large surface area of FeSNPs and partially its decomposition in wet medium to hydrogen sulfide (H_2S) which gives better contact with microorganisms thus alter the microbial metabolism and penetrated inside the microorganisms.

CONCLUSIONS

Green synthesis of iron sulfide nanoparticles FeSNPs is an ecofriendly and safer to environment as compared with chemical and physical methods. A fast, eco-friendly and convenient green method for the synthesis of FeSNPs nanoparticles from iron nitrate nonahydrate and sodium sulfide nonahydrate in aqueous extract of *U. tomentosa*

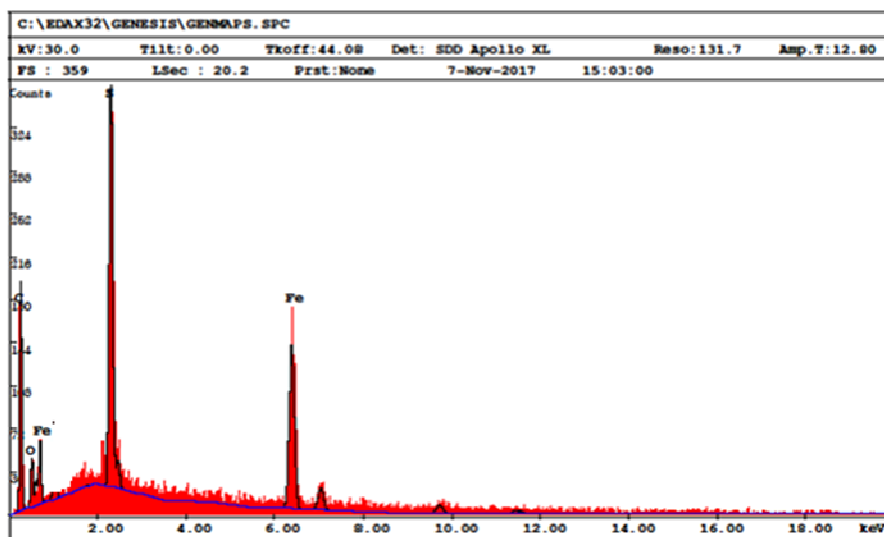


Figure 7 EDS of synthesized FeSNPs

leaves at ambient temperature. Spherical, polydispersity of FeSNPs of particle sizes ranging from 5 to 80 nm with an average size of 40 nm are obtained. The green synthesized FeSNPs showed excellent antifungal activity towards plant pathogenic fungus *F. oxysporum* sp. *lycopersici*. From our preliminary results in this research work, we have detected that FeSNPs decomposed partially in wet land to give iron ions (Fe^{+2}), sulfur ions (S^{-2}) and hydrogen sulfide (H_2S). These results could be used in developing novel antifungal agent, which may find potential applications in agricultural field as fungicide and fertilizer.

ACKNOWLEDGMENT

This research work was supported by funding program from Scientific Research Support Fund (SRF-Agr/2/13/2013) Amman, Jordan. Authors are thankful for Royal Scientific Society and the University of Jordan, Jordan for given all facilities to carry out this research.

REFERENCES

- Akhoondi A, Aghaziarati M, Khandan N (2013). Production of highly pure iron disulfide nanoparticles using hydrothermal synthesis method. *Appl Nanosci* 3: 417–422
- Akhtar MS, Alenad A, Malik MA (2015). **Synthesis of mackinawite FeS thin films from acidic chemical baths.** *Mater Sci in Semiconductor Processing* 32: 1-5
- Chin PP, Ding J, Yi JB, Liu BH (2005). Synthesis of FeS_2 and FeS nanoparticles by high-energy mechanical milling and mechanochemical processing. *J Alloys and Compounds* 390: 255–260
- Cummins DR, Russell HB, Jasinski JB, Menon M, Sunkara MK, (2013). Iron sulfide (FeS) nanotubes using sulfurization of hematite nanowires. *Nano Lett* 13: 2423-2430
- Ding L, Fan S, Sun X, Du J, Liu Z, Tao C (2013). Direct preparation of semiconductor iron sulfide nanocrystals from natural pyrite. *RSC Advances*, 3: 4539-4543
- Ghidan AY, Al-Antary TM, Awwad, AM (2016). Green synthesis of copper oxide nanoparticles using *Punica granatum* peels extract: Effect on green peach Aphid. *Environmental Nanotechnology, Monitoring & Management* 6: 95–98.
- Ivantsov RD, Edelman IS, Dubrovsky AA, Zharkov SM, Velikanov DP, Lin C-R, Tseng Y-T, Shih K-Y (2017). Iron sulfide nanoparticles: Preparation, structure, magnetic properties. *J Siberian Federal University. Mathematics & Physics.* 10: 244–247
- Kar S, Chaudhuri S (2005). Synthesis of highly oriented iron sulfide nanowires through solvothermal process. *Mater Lett* 59: 289-66
- Kim E-J, Kim J-H, Azad, A-M, Chang Y-S (2011). Facile synthesis and characterization of Fe/FeS nanoparticles for environmental applications. *ACS Appl Mater Interfaces* 3: 1457–1462
- Kim Y, Lee Y, Roh Y (2015). Microbial synthesis of iron sulfide (FeS) and iron carbonate (FeCO_3) nanoparticles. *J Nanosci Nanotechnol* 15: 5794-5797
- Liu X, Shangguan E, Li J, Ning S, Guo L, Li Q (2017). A novel electrochemical sensor based on FeS anchored reduced graphene oxide nanosheets for simultaneous determination of dopamine and acetaminophen. *Mater Sci and Eng C.* 70: 628–636
- Liu Y, Wenyan W, Wang J, Mirza ZA, Wang T (2016). Optimized (synthesis of FeS nanoparticles with a high Cr(VI) removal capability. *J Nanomaterials* ID 7817296

- Maji SK, Dutta AK, Biswas P, Srivastava DN, Paul P, Mondal A, Adhikary B (2012). Synthesis and characterization of FeS nanoparticles obtained from a dithiocarboxylate precursor complex and their photocatalytic, electrocatalytic and biomimic peroxidase behavior. *Applied Catalysis A: General*. 419-420: 170-177
- Pua F-L, Chia C-H, Zakaria S, Liew T-K, Yarmo MA, Huang N-M (2010). Preparation of transition metal sulfide nanoparticles via hydrothermal route. *Sains Malaysiana*, 39: 243-248
- Xiao S, Li X, Sun W, Guan B, Wang Y (2016). General and facile synthesis of metal sulfide nanostructures: In situ microwave synthesis and application as binder-free cathode for Li-ion batteries. *Chem Eng J* 306: 251–259
- Zhang Y, Du Y, Xu H, Wang Q (2010). Diverse-shaped iron sulfide nanostructures synthesized from a single source precursor approach. *Cryst Eng Comm* 12: 3658–3663
- Zhao Y, Yao L, Qi Y, Sun L, Wu Z (2009). Facile synthesis of micrometer FeS/PVP architectures with the aid of thiourea. *J Sol-Gel Sci Technol* 50: 3–7
- Zhou L, Liu J, Dong F (2017). Spectroscopic study on biological mackinawite (FeS) synthesized by ferric reducing bacteria (FRB) and sulfate reducing bacteria (SRB): Implications for in-situ remediation of acid mine drainage. *Spectrochimica Acta Part A: Molecular and Biomolecular Spectroscopy* 173: 544-548